NTNU
Innovation and Creativity

Modeling of transmitted and reflected waves in layered media

A. Tantsereva, B. Ursin, N. Favretto-Cristini, P. Cristini, D. Komatitsch and A.M. Aizenberg

22. april 2013
ROSE meeting

Outline

1. Introduction
2. Multiple Tip-Wave Superposition Method
3. Experiment
4. Numerical modeling
   - Narrow-beam experiment
   - Broad-beam experiment
5. Conclusions and future work

Outline

Outline

1. Introduction
2. Multiple Tip-Wave Superposition Method
3. Experiment
4. Numerical modeling
   - Narrow-beam experiment
   - Broad-beam experiment
5. Conclusions and future work

Outline

Outline

Motivation

- 3D seismic modeling is an important tool today.
- Difficulties in simulating 3D wave propagation due to the presence of shadow zones, head waves, diffractions and edge effects.
- How to check the validity of the results?

Synthetic data vs. Laboratory data

- Numerical seismic modeling carried out using the multiple version of the Tip-wave Superposition Method (Ayzenberg et al., 2007 Geophysics 72)
- Laboratory data obtained in the Laboratoire de Mécanique et d'Acoustique in Marseille, France (N. Favretto-Cristini, P. Cristini) for zero-offset experiment in a water tank

Synthetic data vs. Laboratory data

- Numerical seismic modeling carried out using the multiple version of the Tip-wave Superposition Method (Ayzenberg et al., 2007 Geophysics 72)
- Laboratory data obtained in the Laboratoire de Mécanique et d'Acoustique in Marseille, France (N. Favretto-Cristini, P. Cristini) for zero-offset experiment in a water tank

Outline

Multiple Tip-Wave Superposition method

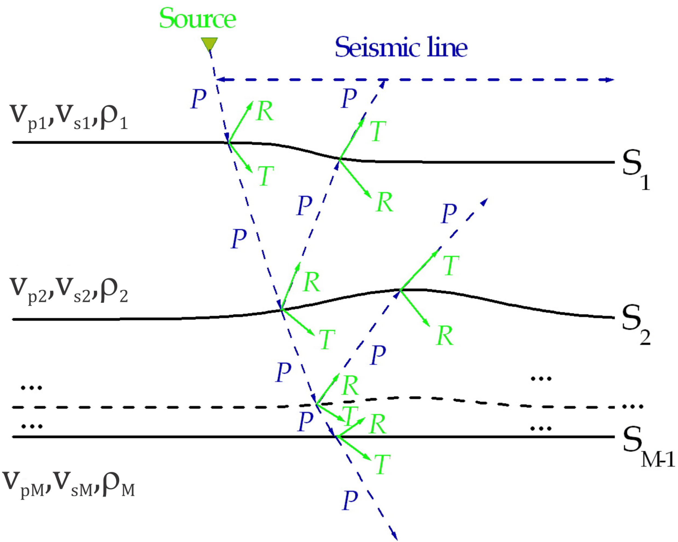

Multiple Tip-Wave Superposition method

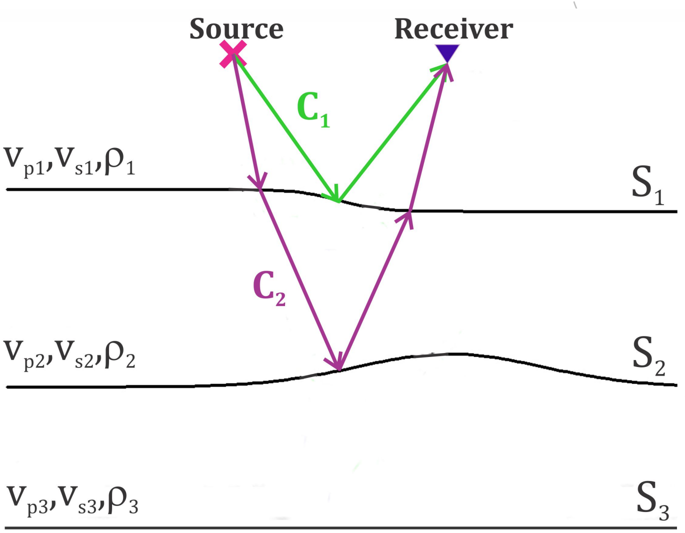

Multiple Tip-Wave Superposition Method

- Superposition of events according to their wavecodes

$$p(\mathbf{x}^r) = p^{(1)}(\mathbf{x}^r) + p^{(3)}(\mathbf{x}^r) \qquad (1)$$

- Combination of surface integral propagators **P** and R/T operators

$$\begin{aligned} p^{(1)}(\mathbf{x}^r) &= \mathrm{P}_{1\mathbf{x}^r}\langle \mathrm{R}_{11}\langle p^{(0)}\rangle\rangle, && (2) \\ p^{(3)}(\mathbf{x}^r) &= \mathrm{P}_{1\mathbf{x}^r}\left\langle \mathrm{T}_{12}\mathrm{P}_{21}\left\langle \mathrm{R}_{22}\mathrm{P}_{12}\langle \mathrm{T}_{12}\langle p^{(0)}\rangle\rangle\right\rangle\right\rangle, && (3) \end{aligned}$$

where $\mathbf{P}(s, s')\langle\ldots\rangle = \frac{1}{4\pi}\iint_{\Sigma}\left[\frac{\partial G(\mathbf{s};\mathbf{s}')}{\partial\mathbf{n}}\langle\ldots\rangle - G(\mathbf{s};\mathbf{s}')\frac{\partial}{\partial\mathbf{n}}\langle\ldots\rangle\right] d\Sigma$
is the propagation operator inside the layer,
R and T are the R/T operators at the interfaces.

Multiple Tip-Wave Superposition Method

Approximations:

1. R/T operators approximated by R/T coefficients $\hat{\mathbf{R}}$ and $\hat{\mathbf{T}}$.
2. Interfaces split into small elements, propagation operators approximated by propagation matrices $\mathbf{L}_{12}$ and $\mathbf{L}_{21}$

Then

$$p^{(1)}(\mathbf{x}^r) \approx \mathrm{P}_{1\mathbf{x}^r} \cdot \mathrm{R}_{11} \cdot p^{(0)}, \quad (4)$$

$$p^{(3)}(\mathbf{x}^r) \approx \mathrm{P}_{1\mathbf{x}^r} \cdot \mathrm{L}_{12} \cdot \mathrm{L}_{21} \cdot \mathrm{T}_{12} \cdot p^{(0)}, \quad (5)$$

where scalar elements of layer matrices $\mathbf{L}_{12}$ and $\mathbf{L}_{21}$ are represented by the tip-wave beams

$$\triangle \mathrm{L} = R/T \cdot \triangle \mathrm{P} = R/T \cdot \left(\frac{-ik}{2\pi} \frac{\triangle \Sigma}{R} \cos \Theta e^{ikR} \right). \quad (6)$$

MTWSM algorithm

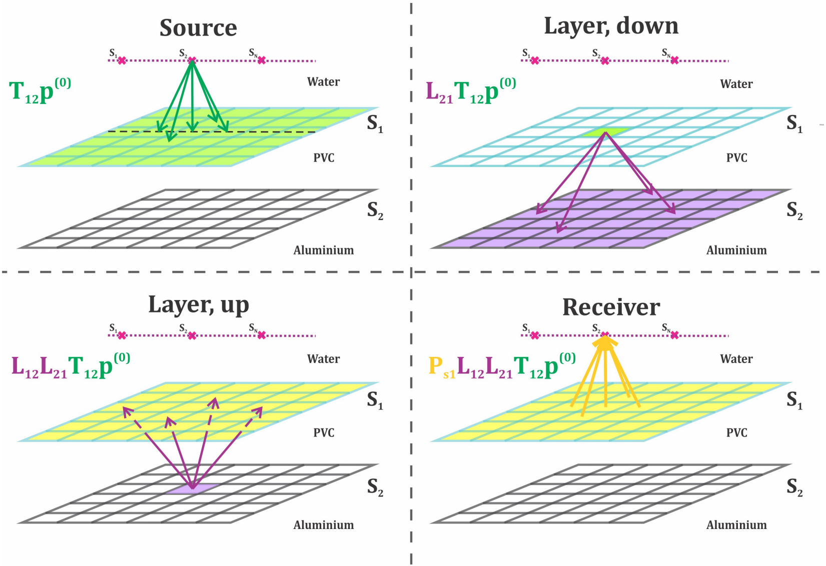

Attenuation

- Characterized by the quality factors Q_p and Q_s.
- Has two different effects on the propagating wave fields:
  - Decrease in amplitude and broadening of a pulse.
  - Change of the impulse shape as reflection/transmission coefficients are functions of the Q-contrast between media.

Attenuation

- Characterized by the quality factors Q_p and Q_s.
- Has two different effects on the propagating wave fields:
  - Decrease in amplitude and broadening of a pulse.
  - Change of the impulse shape as reflection/transmission coefficients are functions of the Q-contrast between media.

Attenuation

- Characterized by the quality factors Q_p and Q_s.
- Has two different effects on the propagating wave fields:
  - Decrease in amplitude and broadening of a pulse.
  - Change of the impulse shape as reflection/transmission coefficients are functions of the Q-contrast between media.

Attenuation

- Characterized by the quality factors Q_p and Q_s.
- Has two different effects on the propagating wave fields:
  - Decrease in amplitude and broadening of a pulse.
  - Change of the impulse shape as reflection/transmission coefficients are functions of the Q-contrast between media.

Kolsky-Futterman model (*Kolsky,1956; Futterman, 1962*)

Assumption: attenuation is strictly linear with frequency over the seismic frequency range (1-200 Hz)

- complex number $k(\omega) = \frac{\omega}{c(\omega)} = \frac{\omega}{c_p(\omega)} + i\alpha(\omega)$
- phase velocity $\frac{1}{c_p(\omega)} = \frac{1}{c_r} + \frac{1}{\pi c_r Q_r} \ln \left| \frac{\omega_r}{\omega} \right|$
- attenuation $\alpha(\omega) = \frac{|\omega|}{2 c_r Q_r}$

where c_r and Q_r are the values of c_p and Q_p at the reference frequency ω_r.

Kolsky-Futterman model (*Kolsky,1956; Futterman, 1962*)

Assumption: attenuation is strictly linear with frequency over the seismic frequency range (1-200 Hz)

- complex number $k(\omega) = \frac{\omega}{c(\omega)} = \frac{\omega}{c_p(\omega)} + i\alpha(\omega)$
- phase velocity $\frac{1}{c_p(\omega)} = \frac{1}{c_r} + \frac{1}{\pi c_r Q_r} \ln\left|\frac{\omega_r}{\omega}\right|$
- attenuation $\alpha(\omega) = \frac{|\omega|}{2c_r Q_r}$

where c_r and Q_r are the values of c_p and Q_p at the reference frequency ω_r.

Kolsky-Futterman model (*Kolsky,1956; Futterman, 1962*)

Assumption: attenuation is strictly linear with frequency over the seismic frequency range (1-200 Hz)

- complex number $k(\omega) = \frac{\omega}{c(\omega)} = \frac{\omega}{c_p(\omega)} + i\alpha(\omega)$
- phase velocity $\frac{1}{c_p(\omega)} = \frac{1}{c_r} + \frac{1}{\pi c_r Q_r} \ln\left|\frac{\omega_r}{\omega}\right|$
- attenuation $\alpha(\omega) = \frac{|\omega|}{2c_r Q_r}$

where c_r and Q_r are the values of c_p and Q_p at the reference frequency ω_r.

Kolsky-Futterman model (*Kolsky,1956; Futterman, 1962*)

Assumption: attenuation is strictly linear with frequency over the seismic frequency range (1-200 Hz)

- complex number $k(\omega) = \frac{\omega}{c(\omega)} = \frac{\omega}{c_p(\omega)} + i\alpha(\omega)$
- phase velocity $\frac{1}{c_p(\omega)} = \frac{1}{c_r} + \frac{1}{\pi c_r Q_r} \ln\left|\frac{\omega_r}{\omega}\right|$
- attenuation $\alpha(\omega) = \frac{|\omega|}{2c_r Q_r}$

where c_r and Q_r are the values of c_p and Q_p at the reference frequency ω_r.

Outline

Marseille model

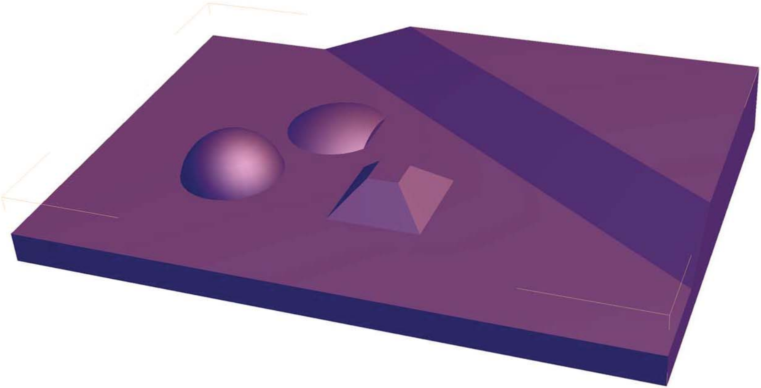

Experiment

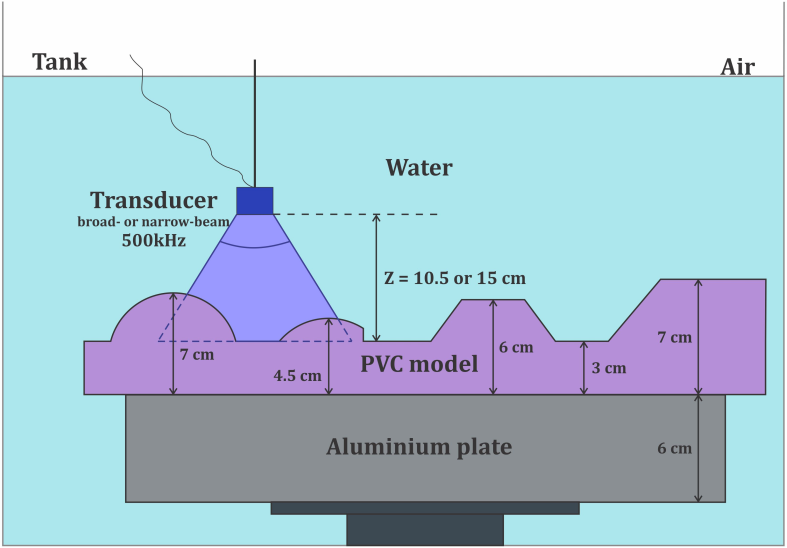
Tank
Air
Water
Transducer
broad- or narrow-beam
500kHz
Z = 10.5 or 15 cm
7 cm
4.5 cm
PVC model
6 cm
3 cm
7 cm
Aluminium plate
6 cm

Properties of the materials

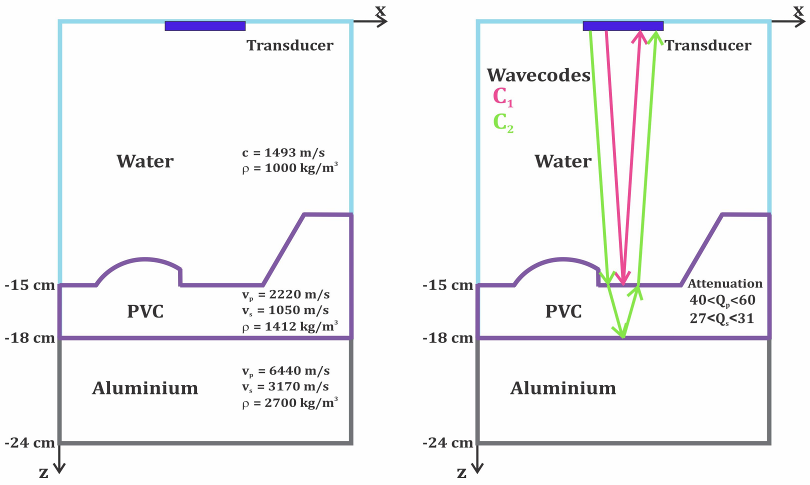

Narrow-beam transducer

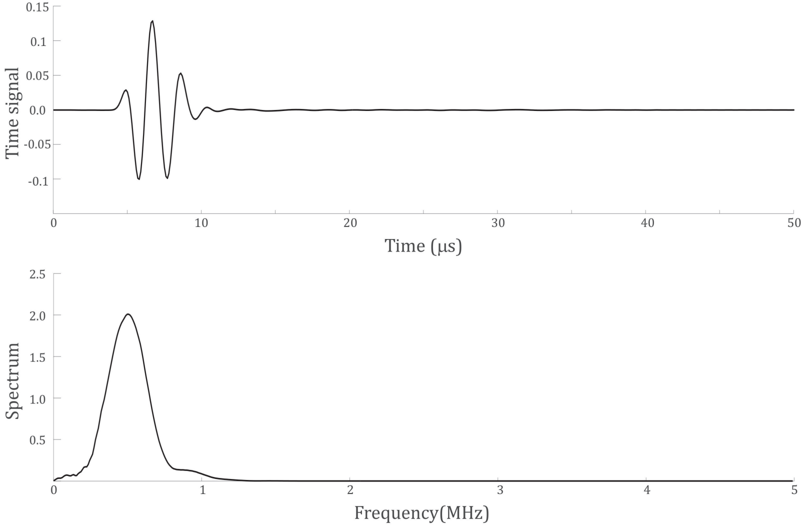

Broad-beam transducer

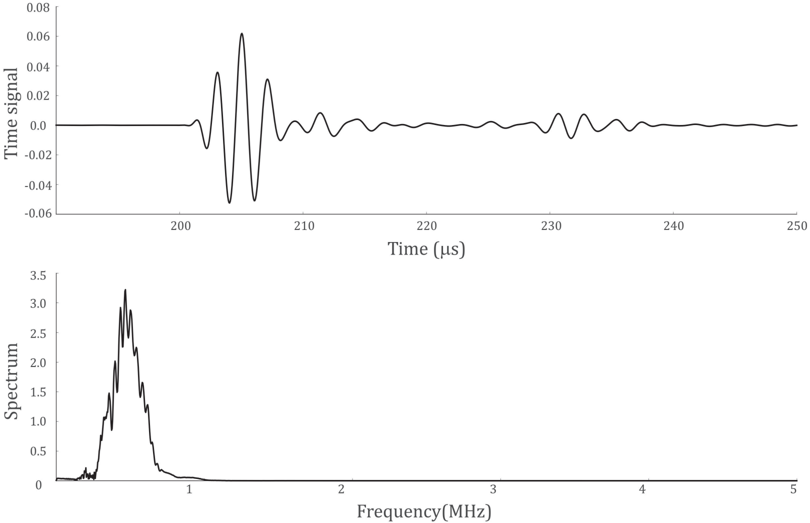

Directivity pattern

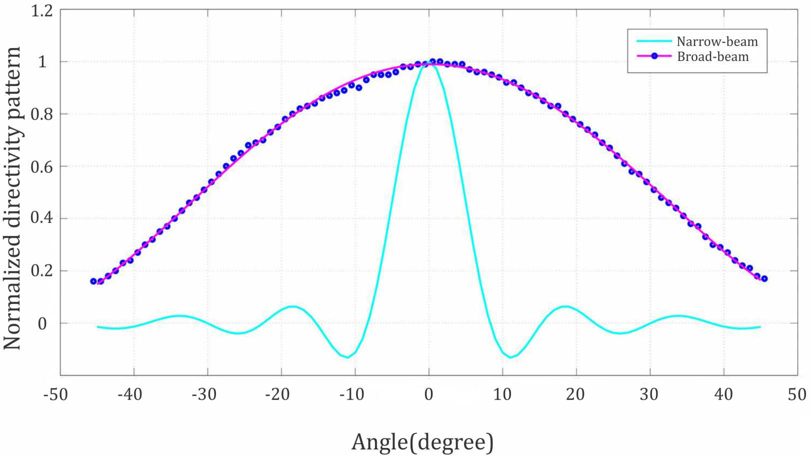

Acquisition design

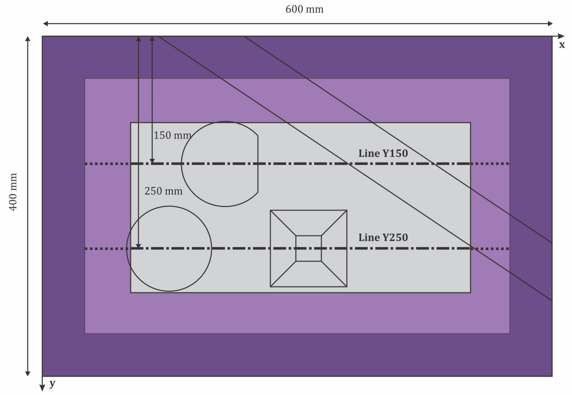

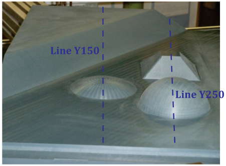

Outline

Line Y150, seismograms

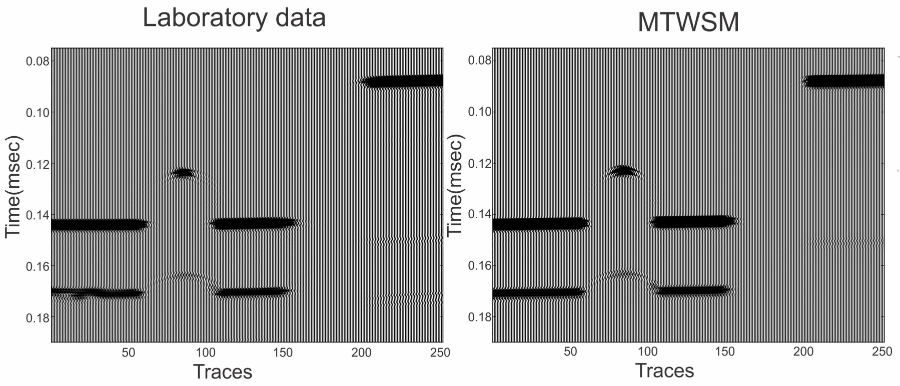

Line Y150, traces

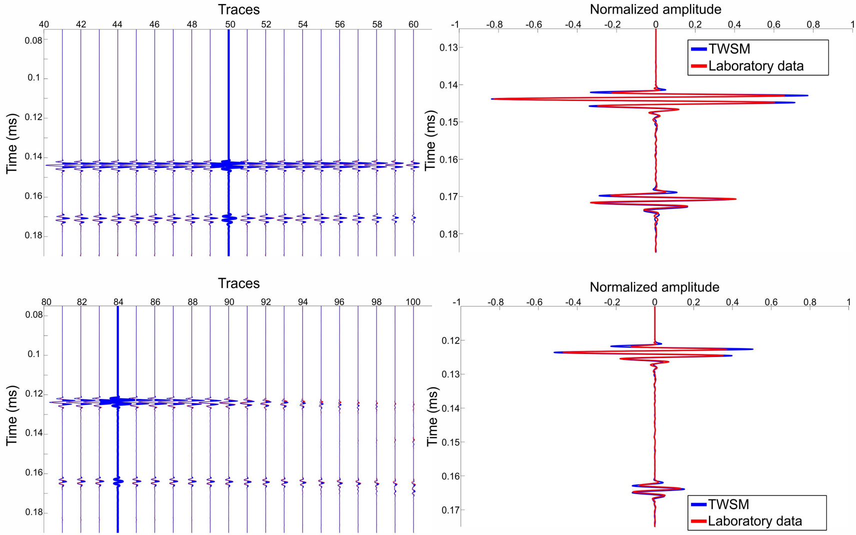

Line Y250, seismograms

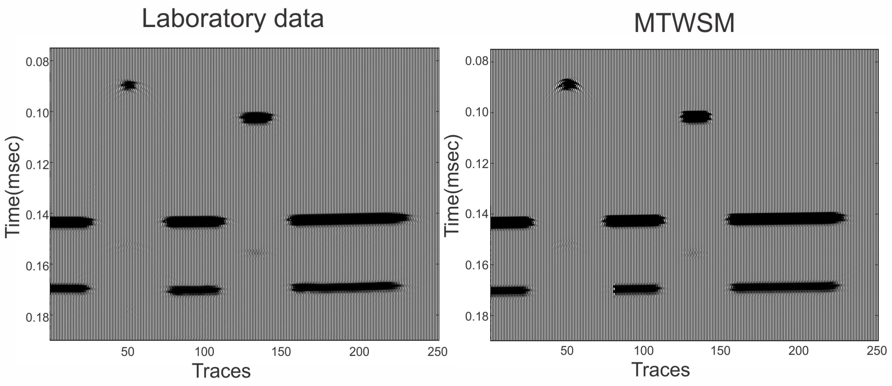

Line Y250, traces

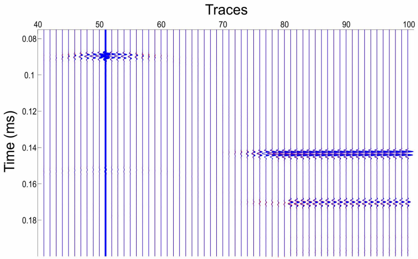

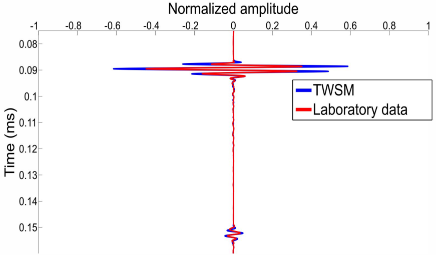

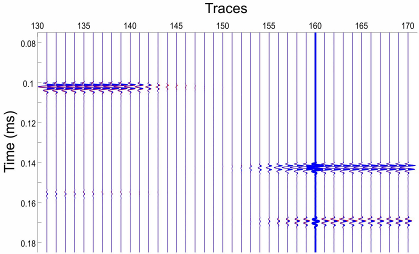

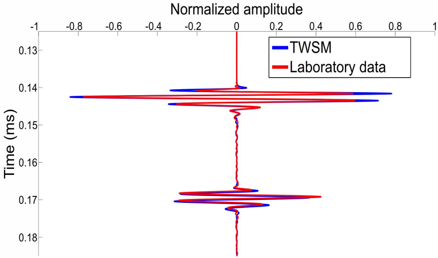

Line Y150, seismograms

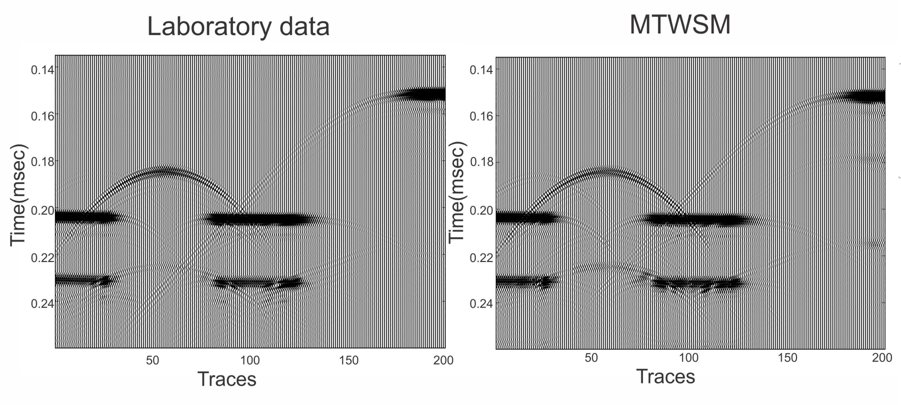

Line Y150, traces

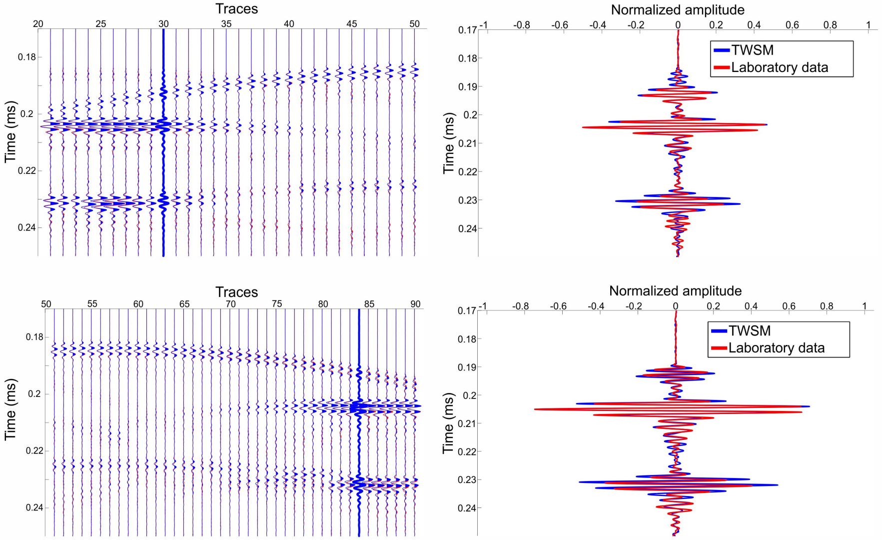

Line Y250, seismograms

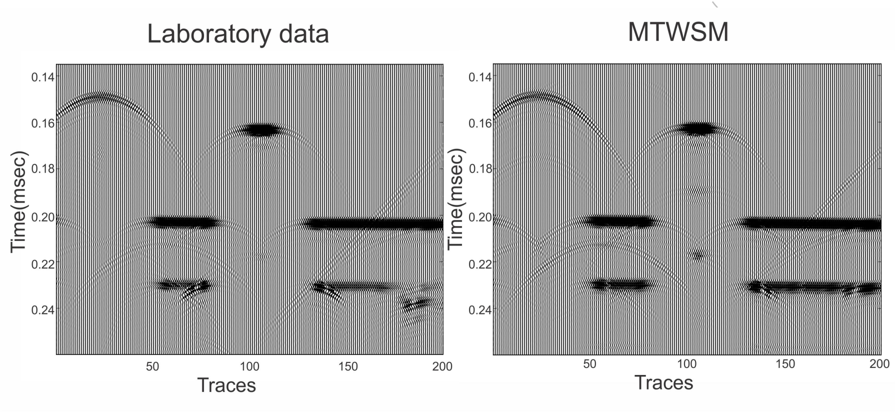

Line Y250, traces

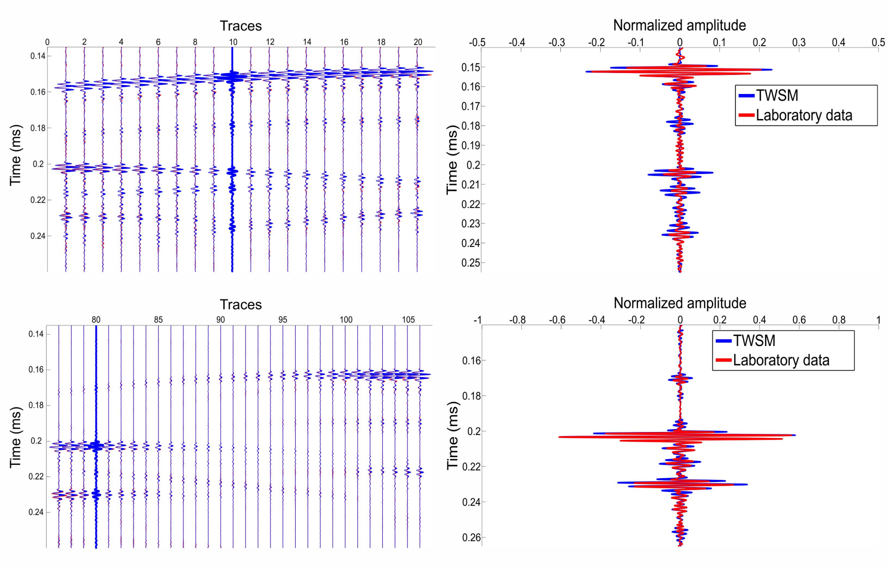

Numerical comparison

Similarity factor $F = 2 \cdot \frac{\sum_t s_1(t) \cdot s_2(t)}{\sum_t s_1^2(t) + \sum_t s_2^2(t)}$.

	Line	**Source 1**	**Source 2**
NB	**Y150**	0.9729	0.9450
	Y250	0.9076	0.9299
BB	**Y150**	0.91860	0.8367
	Y250	0.9158	0.9389

Conclusions and future work

- Numerical simulations of wave propagation in layered medium using the MTWSM.
- Laboratory measurements of reflected ultrasonic waves for narrow-beam and broad-beam transducers.
- Comparisons indicate a good quantitative fit in time arrivals and amplitudes.
- Multi-offset seismic experiments using sources with unfocused beam and 3D array receivers covering the entire model.

Conclusions and future work

- Numerical simulations of wave propagation in layered medium using the MTWSM.
- Laboratory measurements of reflected ultrasonic waves for narrow-beam and broad-beam transducers.
- Comparisons indicate a good quantitative fit in time arrivals and amplitudes.
- Multi-offset seismic experiments using sources with unfocused beam and 3D array receivers covering the entire model.

Conclusions and future work

- Numerical simulations of wave propagation in layered medium using the MTWSM.
- Laboratory measurements of reflected ultrasonic waves for narrow-beam and broad-beam transducers.
- Comparisons indicate a good quantitative fit in time arrivals and amplitudes.
- Multi-offset seismic experiments using sources with unfocused beam and 3D array receivers covering the entire model.

Conclusions and future work

- Numerical simulations of wave propagation in layered medium using the MTWSM.
- Laboratory measurements of reflected ultrasonic waves for narrow-beam and broad-beam transducers.
- Comparisons indicate a good quantitative fit in time arrivals and amplitudes.
- Multi-offset seismic experiments using sources with unfocused beam and 3D array receivers covering the entire model.

Acknowledgements

We thank INSIS Institute of the French CNRS, the Aix-Marseille University, the Carnot Star Institute, Statoil Petroleum AS and the Norwegian Research Council through the ROSE project for financial support and Stephan Devic (LMA Marseille) for making the Marseille model.